Investigation of traveling wave solutions of nonlinear mathematical models by the modified exponential function method

Çağlar KUBAL[1,*], Tolga AKTÜRK[2]

[1] Ordu University, Department of Mathematics, Faculty of Arts and Sciences, Ordu.
[2] Ordu University, Faculty of Education, Department of Mathematics and Science Education, Ordu.

Abstract

In this work, traveling wave solutions of (1+1)-dimensional Landau-Ginzburg-Higgs and Duffing nonlinear partial differential equations, which are examples of mathematical modeling, are obtained and analyzed using the modified exponential function method. In order to facilitate the physical interpretation of the mathematical models represented by these equations, simulations of the behavior of the mathematical model as three-dimensional, contour, density and two-dimensional graphics are given using a package program with the help of appropriate parameters. It has been shown that the modified exponential function method effectively investigates the solutions of (1+1)-dimensional Landau-Ginzburg-Higgs and Duffing equations.

***Keywords:** Traveling wave solutions, (1+1)-dimensional Landau-Ginzburg-Higgs equation, Duffing equation, the modified exponential function method.*

Lineer olmayan matematiksel modellerin hareketli dalga çözümlerinin genişletilmiş üstel fonksiyon metodu kullanılarak incelenmesi

Öz

Bu çalışmada, matematiksel modelleme örnekleri olan (1+1)-boyutlu Landau-Ginzburg-Higgs ve Duffing doğrusal olmayan kısmi diferansiyel denklemlerin yürüyen dalga çözümleri elde edilmiş ve genişletilmiş üstel fonksiyon metodu kullanılarak analiz edilmiştir. Bu denklemlerin temsil ettiği matematiksel modellerin fiziksel yorumunu kolaylaştırmak için uygun parametreler yardımıyla bir paket program kullanılarak

*Çağlar KUBAL, kubalcaglar@gmail.com, https://orcid.org/0000-0003-2958-7514
Tolga AKTÜRK, tolgaakturkk@gmail.com, https://orcid.org/0000-0002-8873-0424

matematiksel modelin davranışının üç boyutlu, kontur, yoğunluk ve iki boyutlu grafikleri olarak simülasyonları verilmiştir. Genişletilmiş üstel fonksiyon metodunun (1+1)-boyutlu Landau-Ginzburg-Higgs ve Duffing denklemlerinin çözümlerinin araştırılmasında etkili bir yöntem olduğu gösterilmiştir.

Anahtar kelimeler: *Yürüyen dalga çözümleri, (1+1)-ölçülü Landau-Ginzburg-Higgs denklemi, Duffing denklemi, genişletilmiş üstel fonksiyon metodu.*

1. Introduction

The mathematical models, understanding and interpreting phenomena related to physics, chemistry, biology, engineering, fluid mechanics, ocean engineering, and health have been an advantage. By investigating the solutions of nonlinear partial differential equations, an example of mathematical modeling, depending on different parameters, it has become easier to comprehend and interpret various events. Therefore, the search for analytical solutions to nonlinear partial differential equations used as mathematical modeling has become an increasingly important research area. Various methods exist in the literature to solve such equations [1-7].

The Landau-Ginzburg-Higgs equation founded by Lev Davidovich Landau and Vitaly Lazarevich Ginzburg explains superconductivity in a radially inhomogeneous plasma and entrained cyclotron waves for coherent ion-cyclotron waves [8]. The Duffing equation is a nonlinear quadratic differential equation used to model certain damped and driven oscillators [9]. It is important to investigate the solutions of these two important equations with a different method and bring them to the literature. When the literature is analyzed, solutions of (1+1) dimensional Landau-Ginzburg-Higgs equation and Duffing equation have been obtained by various methods. (1+1)-dimensional Landau-Ginzburg-Higgs equation: the improved Bernoulli sub-equation function method (IBSEFM) [11], first integral method [12], the tanh function method [13], the multi-symplectic Runge-Kutta method [14], $(G'/G, 1/G)$-expansion method [15], the solitary wave ansatz method [16]. Duffing equation: first integral method [12], Jacobi elliptic functions [17], Daftardar-Jafari method (DJM) [18], exp-function method [19], improved Taylor matrix method [20], the quotient trigonometric function expansion method [21], differential transform method [22]. It has been observed that the solution functions get in this paper are different from the functions found in the above studies and this has contributed to the literature to obtain the traveling wave solutions of these equations.

2. Method

2.1. The modified exponential function method
In this section, information about the modified exponential function method is given and the method is introduced:

$$P(u, u_x, u_t, u_{xx}, u_{tx}, u_{xxx}, \dots) = 0, \qquad (2.1.1)$$

in view of the general expression of the nonlinear partial differential equation, if an unknown function $u = u(x, t)$ is accepted to find the wave solutions of this equation, the wave transform is applied to the equation (2.1.1) as follows:

$$u(x,t) = u(\xi), \qquad \xi = k(x - ct). \tag{2.1.2}$$

In order to find the necessary derivative terms for the equation (2.1.1), the derivatives with respect to ξ are taken in the wave transform (2.1.2). If these terms are substituted in the equation (2.1.1):

$$N(u, u^2, u', u'', \dots) = 0, \tag{2.1.3}$$

the general term of the nonlinear ordinary differential equation is obtained. It is assumed that the solution function u of this equation is as follows:

$$u = \frac{\sum_{i=0}^{p} A_i [e^{-\vartheta(\xi)}]^i}{\sum_{j=0}^{q} B_j [e^{-\vartheta(\xi)}]^j} = \frac{A_0 + A_1 e^{-\vartheta(\xi)} + A_2 e^{-2\vartheta(\xi)} + \dots + A_p e^{-p\vartheta(\xi)}}{B_0 + B_1 e^{-\vartheta(\xi)} + B_2 e^{-2\vartheta(\xi)} + \dots + B_q e^{-q\vartheta(\xi)}}. \tag{2.1.4}$$

Here, $A_i, B_j (0 \le i \le p, 0 \le j \le q)$ are the coefficients. To get the coefficients p and q, the balancing principle between the highest order nonlinear term in equation (2.1.3) and the term with the highest derivative is used. In this way, the limits of equation (2.1.4) are determined.
The ϑ function used in the method is in the form:

$$\vartheta'(\xi) = e^{-\vartheta(\xi)} + \mu e^{\vartheta(\xi)} + \lambda. \tag{2.1.5}$$

This equation has the following families of solutions according to the states of the roots. Where λ and μ are constants to be determined later. [10]:

Family 1: $\lambda^2 - 4\mu > 0, \mu \ne 0,$

$$\vartheta(\xi) = \ln\left(\frac{-\sqrt{\lambda^2 - 4\mu}}{2\mu} \tanh\left(\frac{\sqrt{\lambda^2 - 4\mu}}{2}(\xi + E)\right) - \frac{\lambda}{2\mu}\right). \tag{2.1.6}$$

Family 2: $\lambda^2 - 4\mu < 0, \mu \ne 0,$

$$\vartheta(\xi) = \ln\left(\frac{\sqrt{-\lambda^2 + 4\mu}}{2\mu} \tan\left(\frac{\sqrt{-\lambda^2 + 4\mu}}{2}(\xi + E)\right) - \frac{\lambda}{2\mu}\right). \tag{2.1.7}$$

Family 3: $\lambda^2 - 4\mu > 0, \lambda \ne 0, \mu = 0,$

$$\vartheta(\xi) = -\ln\left(\frac{\lambda}{e^{\lambda(\xi+E)} - 1}\right). \tag{2.1.8}$$

Family 4: $\lambda^2 - 4\mu = 0, \lambda \ne 0, \mu \ne 0,$

$$\vartheta(\xi) = \ln\left(-\frac{2\lambda(\xi + E) + 4}{\lambda^2(\xi + E)}\right). \tag{2.1.9}$$

Family 5: $\lambda^2 - 4\mu = 0, \lambda = 0, \mu = 0,$

$$\vartheta(\xi) = \ln(\xi + E). \tag{2.1.10}$$

Where E is an integral constant. After the limits of equation (2.1.4) are determined by the balancing principle as explained above, the necessary derivative terms are obtained and written into the equation (2.1.3). As a result, when the $e^{-\vartheta(\xi)}$ exponential function is classified, a system of equations consisting of $A_0, A_1, A_2, \dots A_p,, B_0, B_1, \dots, B_q$ coefficients is obtained. When this system of equations is solved with a package program,

the coefficients $A_0, A_1, A_2, \dots A_p,, B_0, B_1, \dots, B_q$ in equation (2.1.4) are get. These coefficients and the $\vartheta(\xi)$ functions in the solution families are written together in the equation (2.1.4), and the solution functions are found. It is shown with the package program that these solution functions provide both the ordinary differential equation and the partial differential equation. Thus, the traveling wave solution functions of the nonlinear partial differential equation, the mathematical model are found.

3. Application of the method

3.1. (1+1)-dimensional Landau-Ginzburg-Higgs equation
In this section, by applying wave transform to (1+1)-dimensional Landau-Ginzburg-Higgs equation, traveling wave solutions are obtained with the modified exponential function method.
The (1+1)-dimensional Landau-Ginzburg-Higgs equation looks like this [11]:

$$u_{tt} - u_{xx} - m^2 u + n^2 u^3 = 0. \tag{3.1.1}$$

Later tha $u(x,t) = u(\xi), \ \xi = k(x - ct)$n wave transform is done, if the derivative terms required for the equation (3.1.1) are found and replaced in the equation, the following nonlinear ordinary differential equation is get to:

$$k^2(c^2 - 1)u'' - m^2 u + n^2 u^3 = 0. \tag{3.1.2}$$

In equation (3.1.2), if the balancing principle is used between the nonlinear highest order term and the term with the highest order derivative:

$u^3 \cong u''$
$p \cong q + 1$
for $q = 1, p = 2$ is obtained. In this case, equation (2.1.4) is as follows:
$$u = \frac{A_0 + A_1 e^{-\vartheta(\xi)} + A_2 e^{-2\vartheta(\xi)}}{B_0 + B_1 e^{-\vartheta(\xi)}}. \tag{3.1.3}$$

If the derivative terms in equation (3.1.2) are obtained from equation (3.1.3) and substituted, the algebraic equation system is found. After this system of equations is solved with the package program and the coefficients are found, the solution functions are obtained according to the situations in the solution family. Three-dimensional, contour, density, and two-dimensional graphics of these solution functions were also drawn with the help of the package program.

Case-1:
$A_0 = \frac{i\sqrt{-1+c^2}k\lambda B_0}{\sqrt{2}n}, A_1 = \frac{i\sqrt{-1+c^2}k(2B_0+\lambda B_1)}{\sqrt{2}n}, A_2 = \frac{i\sqrt{2}\sqrt{-1+c^2}kB_1}{n}, m = \frac{i\sqrt{-1+c^2}k\sqrt{\lambda^2-4\mu}}{\sqrt{2}},$
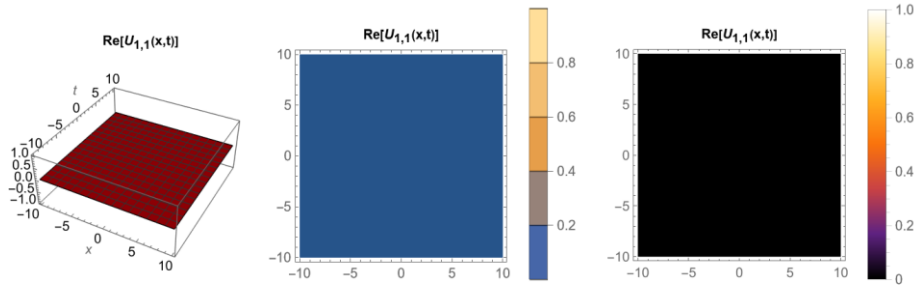with the help of the above coefficients, the solution function u given below is obtained:
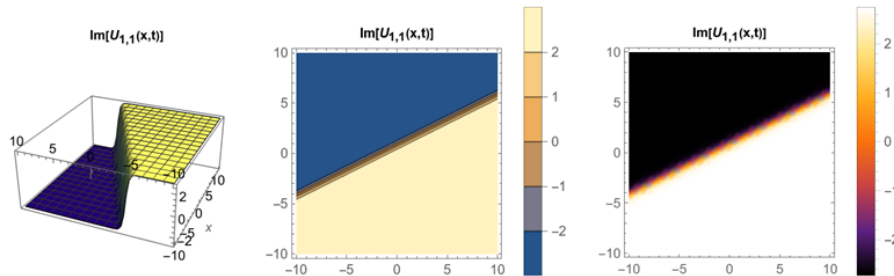$$u_1(x,t) = \frac{i\sqrt{-1+c^2}e^{-\vartheta}k(2+e^{\vartheta}\lambda)}{\sqrt{2}n}, \tag{3.1.4}$$
Family 1: Solution of equation (3.1.1) for $\lambda^2 - 4\mu > 0, \ \mu \neq 0$ and its graphs:
$$u_{1,1}(x,t) = \frac{i\sqrt{-1+c^2}k(\lambda^2 - 4\mu + \lambda\rho)}{\sqrt{2}n(\lambda + \rho)}, \tag{3.1.5}$$
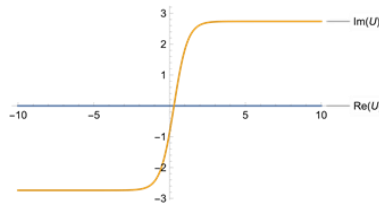
$$\rho = \left[\sqrt{\lambda^2 - 4\mu}\tanh\left[\frac{1}{2}\big(E + k(-ct + x)\big)\sqrt{\lambda^2 - 4\mu}\right]\right].$$
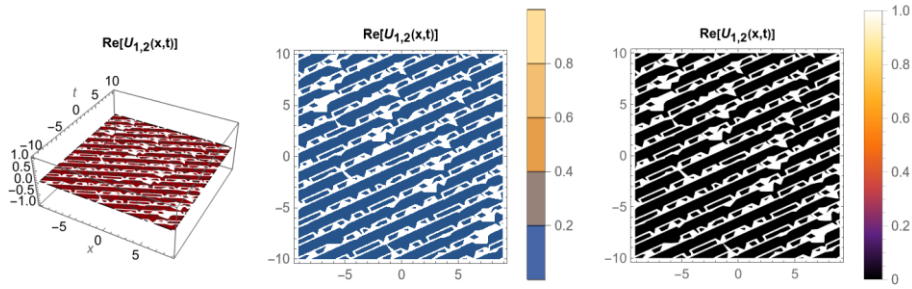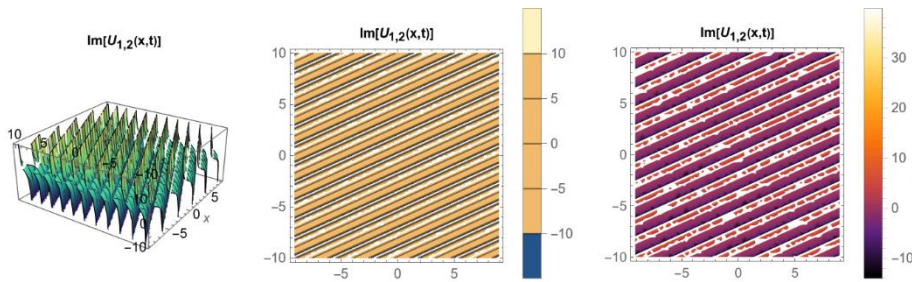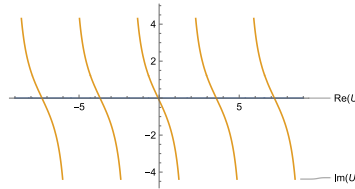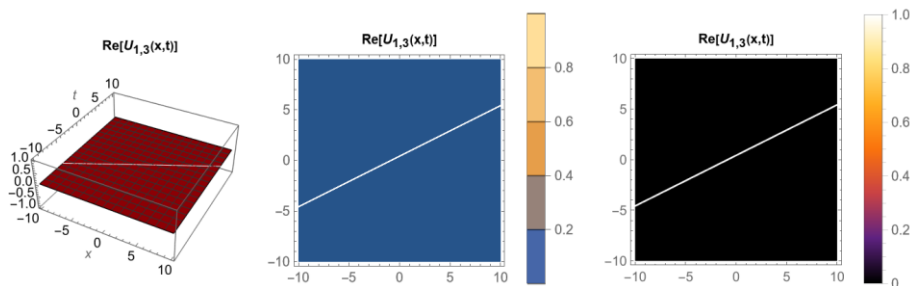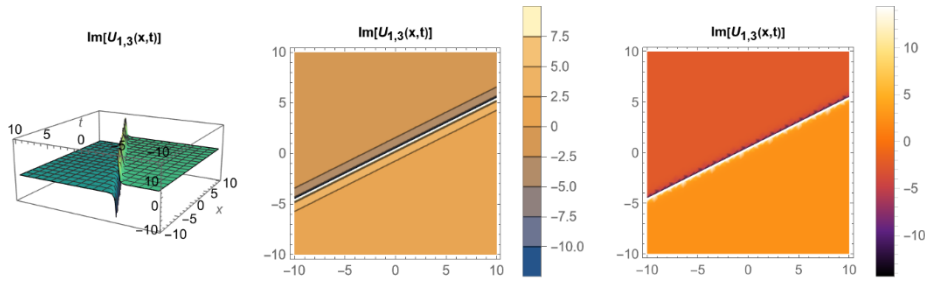

Figure 1. Simulations of the behavior of the model represented by equation (3.1.5) for $k = 1,\ c = 2,\ \lambda = 3,\ \mu = 1,\ m = i\sqrt{\frac{15}{2}},\ n = 1$ and $E = 0.85$
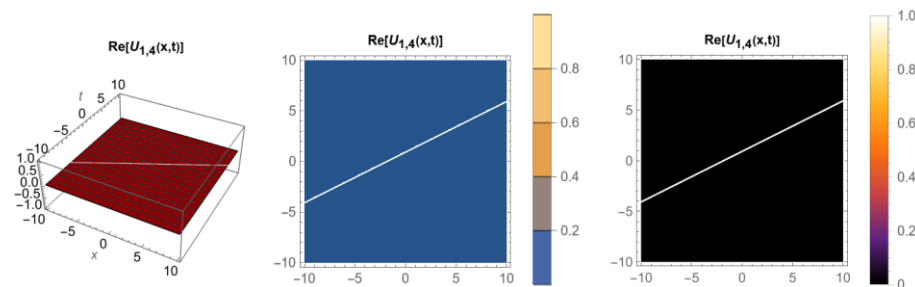

Figure 2. Simulations of the behavior of the model represented by equation (3.1.5) for $k = 1,\ c = 2,\ \lambda = 3,\ \mu = 1,\ m = i\sqrt{\frac{15}{2}},\ n = 1$ and $E = 0.85$

Figure 3. Simulations of the behavior of the model represented by equation (3.1.5) for (3.1.5) for $k = 1,\ c = 2,\ \lambda = 3,\ \mu = 1,\ m = i\sqrt{\frac{15}{2}},\ n = 1,\ E = 0.85$ and $t = 1$

Family 2: Solution of equation (3.1.1) for $\lambda^2 - 4\mu < 0,\ \mu \neq 0$ and its graphs:

$$u_{1,2}(x,t) = \frac{i\sqrt{-1 + c^2}k(\lambda^2 - 4\mu - \lambda\sigma)}{\sqrt{2}n(\lambda - \sigma)}, \tag{3.1.6}$$

$$\sigma = \left[\sqrt{-\lambda^2 + 4\mu}\tan\left[\frac{1}{2}\big(E + k(-ct + x)\big)\sqrt{-\lambda^2 + 4\mu}\right]\right].$$
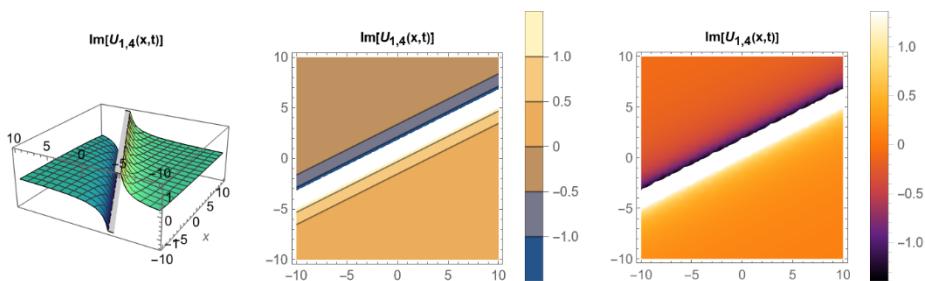
Figure 4. Simulations of the behavior of the model represented by equation (3.1.6) for $k = 1$, $c = 2$, $\lambda = 1$, $\mu = 1$, $m = -\frac{3}{\sqrt{2}}$, $n = 1$ and $E = 0.85$

Figure 5. Simulations of the behavior of the model represented by equation (3.1.6) for $k = 1$, $c = 2$, $\lambda = 1$, $\mu = 1$, $m = -\frac{3}{\sqrt{2}}$, $n = 1$ and $E = 0.85$

Figure 6. Simulations of the behavior of the model represented by equation (3.1.6) for $k = 1$, $c = 2$, $\lambda = 1$, $\mu = 1$, $m = -\frac{3}{\sqrt{2}}$, $n = 1$, $E = 0.85$ and $t = 1$

Family 3: Solution of equation (3.1.1) for $\lambda^2 - 4\mu > 0$, $\lambda \neq 0$, $\mu = 0$ and its graphs:

$$u_{1,3}(x,t) = \frac{i\sqrt{-1 + c^2}\, k\lambda \coth[\tau]}{\sqrt{2}n}, \tag{3.1.7}$$

$\tau = \left[\frac{1}{2}\big(E + k(-ct + x)\big)\lambda\right].$

Figure 7. Simulations of the behavior of the model represented by equation (3.1.7) for $k = 1$, $c = 2$, $\lambda = 2$, $\mu = 0$, $m = i\sqrt{6}$, $n = 1$ and $E = 0.85$

Figure 8. Simulations of the behavior of the model represented by equation (3.1.7) for $k = 1, \ c = 2, \ \lambda = 2, \ \mu = 0, \ m = i\sqrt{6}, \ n = 1$ and $E = 0.85$
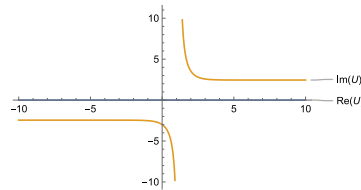
Figure 9. Simulations of the behavior of the model represented by equation (3.1.7) for $k = 1, \ c = 2, \ \lambda = 2, \ \mu = 0, \ m = i\sqrt{6}, \ n = 1, \ E = 0.85$ and $t = 1$

Family 4: Solution of equation (3.1.1) for $\lambda^2 - 4\mu = 0, \ \lambda \neq 0, \ \mu \neq 0$ and its graphs:

$$u_{1,4}(x,t) = \frac{i\sqrt{2}\sqrt{-1 + c^2}k}{n + En - cknt + knx}. \tag{3.1.8}$$

Figure 10. Simulations of the behavior of the model represented by equation (3.1.8) for $k = 1, \ c = 2, \ \lambda = 2, \ \mu = 1, \ m = 0, \ n = 1$ and $E = 0.85$

Figure 11. Simulations of the behavior of the model represented by equation (3.1.8) for $k = 1, \ c = 2, \ \lambda = 2, \ \mu = 1, \ m = 0, \ n = 1$ and $E = 0.85$
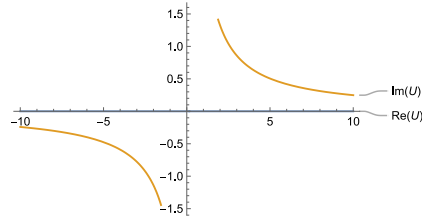
Figure 12. Simulations of the behavior of the model represented by equation (3.1.8) for $k = 1, \ c = 2, \ \lambda = 2, \ \mu = 1, \ m = 0, \ n = 1, \ E = 0.85$ and $t = 1$

Family 5: Solution of equation (3.1.1) for $\lambda^2 - 4\mu = 0, \ \lambda = 0, \ \mu = 0$ and its graphs:
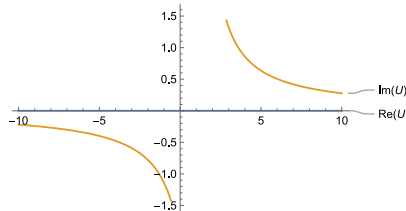
$$u_{1,5}(x,t) = \frac{i\sqrt{2}\sqrt{-1 + c^2}\,k}{n\big(E + k(-ct + x)\big)}. \tag{3.1.9}$$
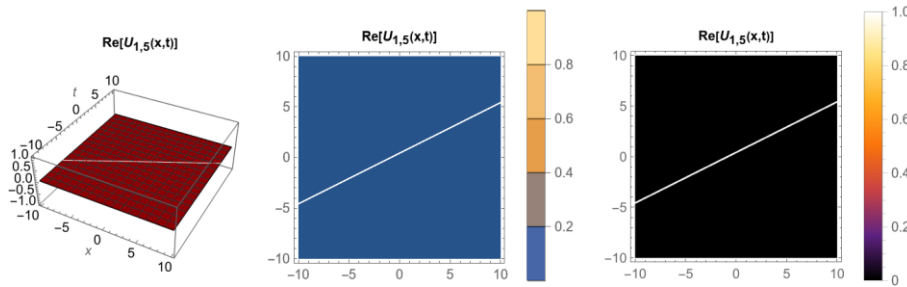
Figure 13. Simulations of the behavior of the model represented by equation (3.1.9) for $k = 1, \ c = 2, \ \lambda = 0, \ \mu = 0, \ m = 0, \ n = 1$ and $E = 0.85$
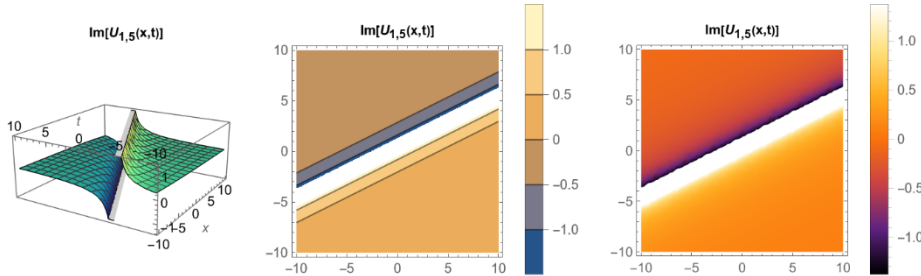
Figure 14. Simulations of the behavior of the model represented by equation (3.1.9) for $k = 1, \ c = 2, \ \lambda = 0, \ \mu = 0, \ m = 0, \ n = 1$ and $E = 0.85$

Figure 15. Simulations of the behavior of the model represented by equation (3.1.9) for $k = 1, \ c = 2, \ \lambda = 0, \ \mu = 0, \ m = 0, \ n = 1, \ E = 0.85$ and $t = 1$

Case-2:

$$A_0 = -\frac{2(-1+c^2)k^2 B_0^2}{n^2 A_2}, A_1 = \frac{2\sqrt{2}\sqrt{-((-1+c^2)k^2)}B_0}{n}, B_1 = \frac{nA_2}{\sqrt{2}\sqrt{-((-1+c^2)k^2)}}, \lambda =$$

$$\frac{2\sqrt{2}\sqrt{-((-1+c^2)k^2)}B_0}{nA_2},$$

582

$$\mu = \frac{m^2}{2(-1+c^2)k^2} - \frac{2(-1+c^2)k^2 B_0^2}{n^2 A_2^2},$$

with the help of these coefficients;

$$u_2(x,t) = \frac{\sqrt{2}e^{-\vartheta}\sqrt{-((-1+c^2)k^2)n - \dfrac{2(-1+c^2)k^2 B_0}{A_2}}}{n^2}, \qquad (3.1.10)$$
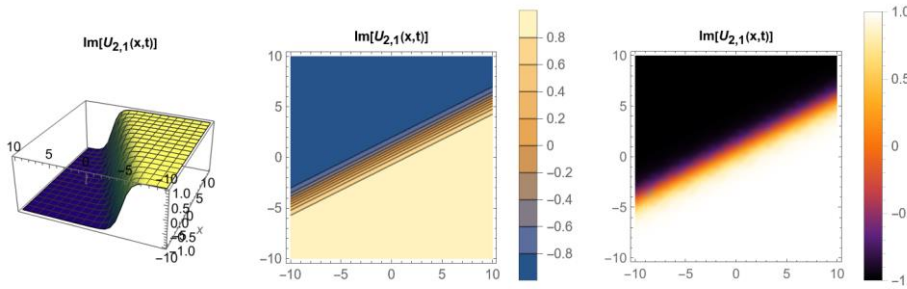
solution function is reached.

Family 1: Solution of equation (3.1.1) for $\lambda^2 - 4\mu > 0$, $\mu \neq 0$ and its graphs:

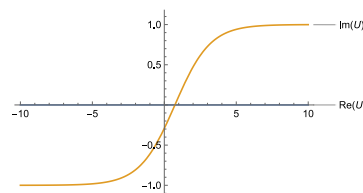$$u_{2,1}(x,t) = \frac{\varphi - \dfrac{2\sqrt{2}\sqrt{-((-1+c^2)k^2)n\mu}}{\lambda + \rho}}{n^2}, \qquad (3.1.11)$$

$$\rho = \left[\sqrt{\lambda^2 - 4\mu}\tanh\left[\frac{1}{2}(E + k(-ct + x))\sqrt{\lambda^2 - 4\mu}\right]\right], \quad \varphi = \left[-\frac{2(-1+c^2)k^2 B_0}{A_2}\right].$$
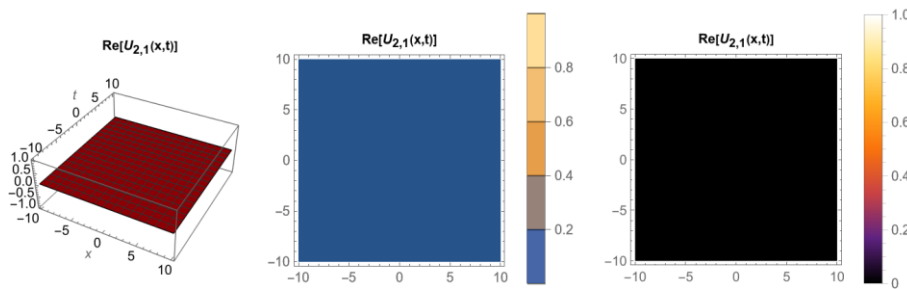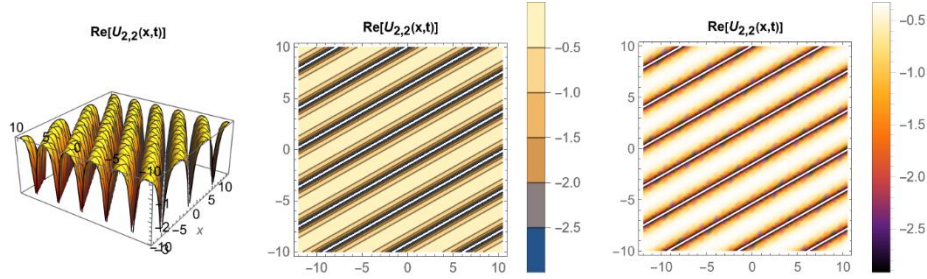

Figure 16. Simulations of the behavior of the model represented by equation (3.1.11) for $A_2 = i$, $B_0 = 1$, $k = 1$, $c = 2$, $m = i$, $n = 1$, $\lambda = 2\sqrt{6}$, $\mu = \frac{35}{6}$ and $E = 0.85$

Figure 17. Simulations of the behavior of the model represented by equation (3.1.11) for $A_2 = i$, $B_0 = 1$, $k = 1$, $c = 2$, $m = i$, $n = 1$, $\lambda = 2\sqrt{6}$, $\mu = \frac{35}{6}$ and $E = 0.85$

Figure 18. Simulations of the behavior of the model represented by equation (3.1.11) for $A_2 = i$, $B_0 = 1$, $k = 1$, $c = 2$, $m = i$, $n = 1$, $\lambda = 2\sqrt{6}$, $\mu = \frac{35}{6}$, $E = 0.85$ and $t = 1$
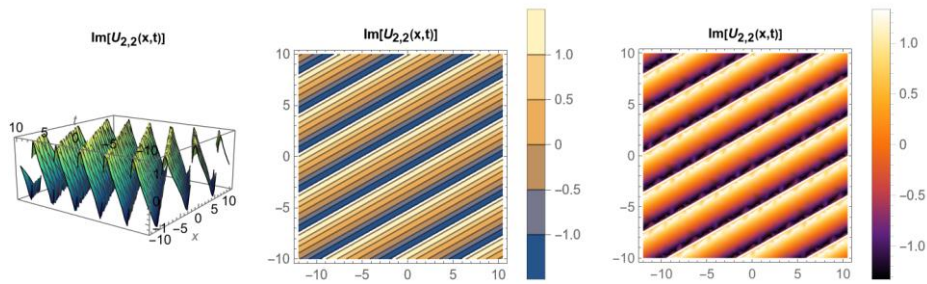
Family 2: Solution of equation (3.1.1) for $\lambda^2 - 4\mu < 0$, $\mu \neq 0$ and its graphs:

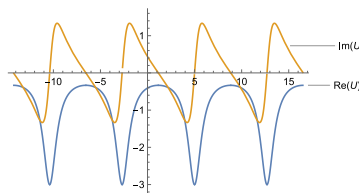$$u_{2,2}(x,t) = \frac{\varphi - \frac{2\sqrt{2}\sqrt{-((-1+c^2)k^2)n\mu}}{\lambda - \sigma}}{n^2},$$ (3.1.12)

$$\sigma = \left[\sqrt{-\lambda^2 + 4\mu}\tan\left[\frac{1}{2}(E + k(-ct + x))\sqrt{-\lambda^2 + 4\mu}\right]\right], \quad \varphi = \left[-\frac{2(-1+c^2)k^2 B_0}{A_2}\right].$$

Figure 19. Simulations of the behavior of the model represented by equation (3.1.12) for $A_2 = 1$, $B_0 = \frac{1}{2}$, $k = 1$, $c = 2$, $m = 1$, $n = 1$, $\lambda = i\sqrt{6}$, $\mu = -\frac{4}{3}$ and $E = 0.85$

Figure 20. Simulations of the behavior of the model represented by equation (3.1.12) for $A_2 = 1$, $B_0 = \frac{1}{2}$, $k = 1$, $c = 2$, $m = 1$, $n = 1$, $\lambda = i\sqrt{6}$, $\mu = -\frac{4}{3}$ and $E = 0.85$

Figure 21. Simulations of the behavior of the model represented by equation (3.1.12) for $A_2 = 1$, $B_0 = \frac{1}{2}$, $k = 1$, $c = 2$, $m = 1$, $n = 1$, $\lambda = i\sqrt{6}$, $\mu = -\frac{4}{3}$, $E = 0.85$ and $t = 1$
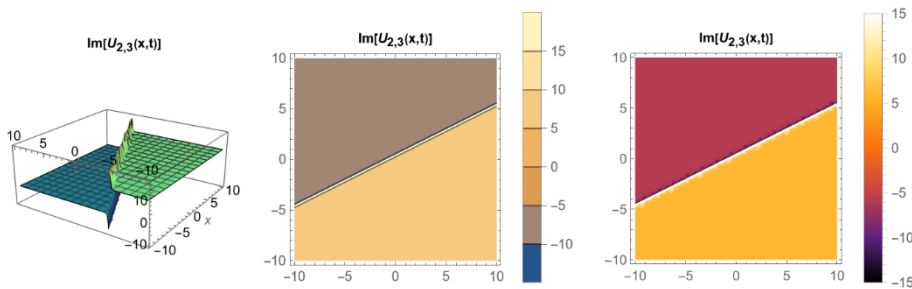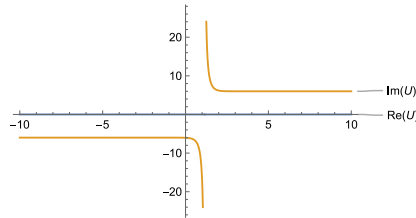
Family 3: Solution of equation (3.1.1) for $\lambda^2 - 4\mu > 0$, $\lambda \neq 0$, $\mu = 0$ and its graphs:

$$u_{2,3}(x,t) = \frac{\frac{\sqrt{2}\sqrt{-((-1+c^2)k^2)n\lambda}}{-1+e^{(E-ckt+kx)\lambda}} + \varphi}{n^2},$$ (3.1.13)

$$\varphi = \left[-\frac{2(-1+c^2)k^2 B_0}{A_2}\right].$$
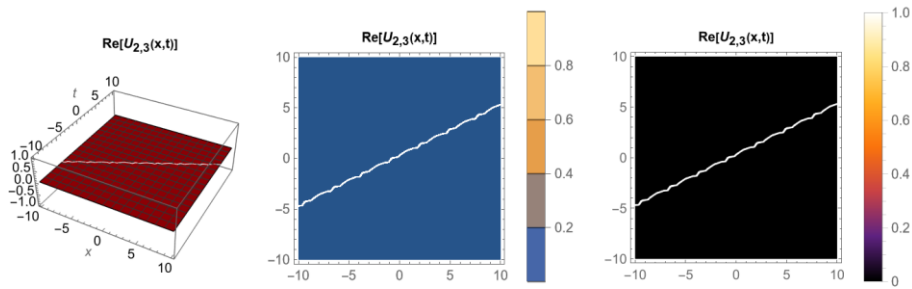
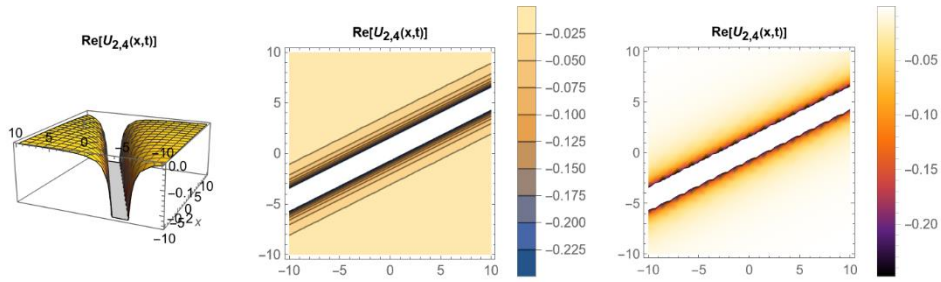**Figure 22.** Simulations of the behavior of the model represented by equation (3.1.13) for $A_2 = 1$, $B_0 = i$, $k = 1$, $c = 2$, $m = 6i$, $n = 1$, $\lambda = -2\sqrt{6}$, $\mu = 0$ and $E = 0.85$

Figure 23. Simulations of the behavior of the model represented by equation (3.1.13) for $A_2 = 1$, $B_0 = i$, $k = 1$, $c = 2$, $m = 6i$, $n = 1$, $\lambda = -2\sqrt{6}$, $\mu = 0$ and $E = 0.85$

Figure 24. Simulations of the behavior of the model represented by equation (3.1.13) for $A_2 = 1$, $B_0 = i$, $k = 1$, $c = 2$, $m = 6i$, $n = 1$, $\lambda = -2\sqrt{6}$, $\mu = 0$, $E = 0.85$ and $t = 1$
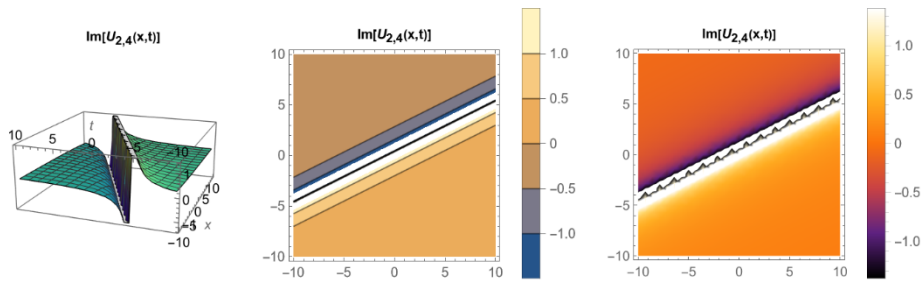
Family 4: Solution of equation (3.1.1) for $\lambda^2 - 4\mu = 0$, $\lambda \neq 0$, $\mu \neq 0$ and its graphs:

$$u_{2,4}(x,t) = \frac{\dfrac{16\sqrt{2}\sqrt{-((-1+c^2)k^2)n(E + k(-ct + x))}}{4 + 8i(E + k(-ct + x))} + \varphi}{n^2}, \qquad (3.1.14)$$
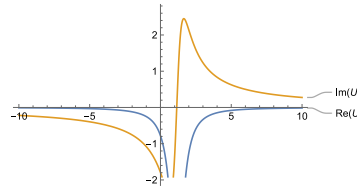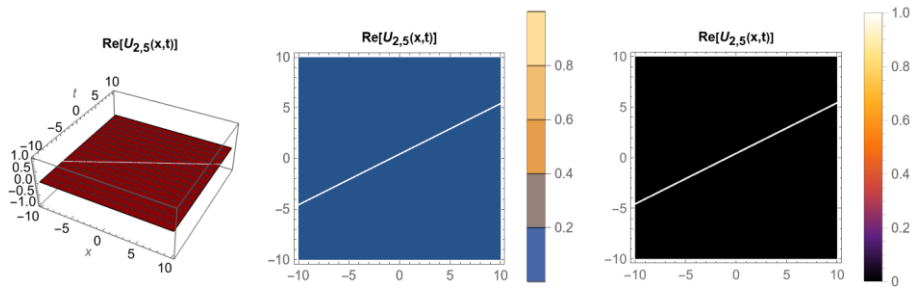
$$\varphi = \left[-\frac{2(-1+c^2)k^2 B_0}{A_2} \right].$$

Figure 25. Simulations of the behavior of the model represented by equation (3.1.14) for $A_2 = 1$, $B_0 = \frac{2}{\sqrt{6}}$, $k = 1$, $c = 2$, $m = 0$, $n = 1$, $\lambda = 4i$, $\mu = -4$ and $E = 0.85$

Figure 26. Simulations of the behavior of the model represented by equation (3.1.14) for $A_2 = 1$, $B_0 = \frac{2}{\sqrt{6}}$, $k = 1$, $c = 2$, $m = 0$, $n = 1$, $\lambda = 4i$, $\mu = -4$ and $E = 0.85$

Figure 27. Simulations of the behavior of the model represented by equation (3.1.14) for $A_2 = 1$, $B_0 = \frac{2}{\sqrt{6}}$, $k = 1$, $c = 2$, $m = 0$, $n = 1$, $\lambda = 4i$, $\mu = -4$, $E = 0.85$ and $t = 1$
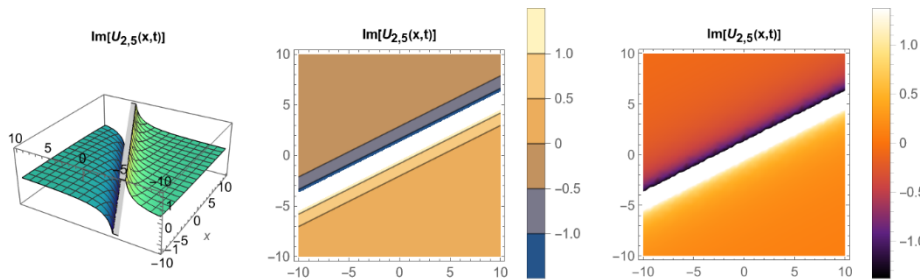
Family 5: Solution of equation (3.1.1) for $\lambda^2 - 4\mu = 0$, $\lambda = 0$, $\mu = 0$ and its graphs:

$$u_{2,5}(x,t) = \frac{\sqrt{2}\sqrt{\dfrac{-\left((-1+c^2)k^2\right)n}{E - ckt + kx}} + \varphi}{n^2},\tag{3.1.15}$$
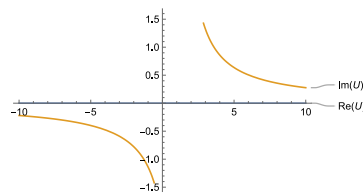
$\varphi = \left[-\dfrac{2(-1+c^2)k^2 B_0}{A_2} \right]$.

Figure 28. Simulations of the behavior of the model represented by equation (3.1.15) for $A_2 = 1$, $B_0 = 0$, $k = 1$, $c = 2$, $m = 0$, $n = 1$, $\lambda = 0$, $\mu = 0$ and $E = 0.85$

Figure 29. Simulations of the behavior of the model represented by equation (3.1.15) for $A_2 = 1$, $B_0 = 0$, $k = 1$, $c = 2$, $m = 0$, $n = 1$, $\lambda = 0$, $\mu = 0$ and $E = 0.85$

Figure 30. Simulations of the behavior of the model represented by equation (3.1.15) for $A_2 = 1$, $B_0 = 0$, $k = 1$, $c = 2$, $m = 0$, $n = 1$, $\lambda = 0$, $\mu = 0$, $E = 0.85$ and $t = 1$

3.2. Duffing equation

In this section, traveling wave solutions are found by using the extended exponential function method by making wave transformation to the Duffing equation.

$$u_{tt} + au + bu^3 = 0. \tag{3.2.1}$$

Duffing equation is as above [12].
After applying the $u(x, t) = u(\xi)$, $\xi = k(x - ct)$ wave transform, if the derivative terms needed for the equation (3.2.1) are obtained and written in the equation:

$$k^2 c^2 u'' + au + bu^3 = 0, \tag{3.2.2}$$

it is degraded to its nonlinear ordinary differential form.
In the equation (3.2.2), if the balancing principle between the nonlinear highest order term and the term with the highest order derivative is analyzed:
$$u^3 \cong u''$$

$p \cong q + 1$

for $q = 1$, $p = 2$ is assumed. In this case, equation (3.1.4) becomes:

$$u = \frac{A_0 + A_1 e^{-\vartheta(\xi)} + A_2 e^{-2\vartheta(\xi)}}{B_0 + B_1 e^{-\vartheta(\xi)}}. \tag{3.2.3}$$

By finding the derivative terms in equation (3.2.2) from equation (3.2.3) and writing them in equation (3.2.2), the algebraic equation system is solved and the solution functions u are obtained according to the solution family. Three-dimensional, contour, density and two-dimensional graphics of these solution functions were also drawn with the package program.

Case-1:

$$A_0 = \frac{i\sqrt{2}ckB_0^2}{\sqrt{b}B_1}, A_1 = \frac{2i\sqrt{2}ckB_0}{\sqrt{b}}, A_2 = \frac{i\sqrt{2}ckB_1}{\sqrt{b}}, a = \frac{2c^2k^2(B_0^2 - \mu B_1^2)}{B_1^2}, \lambda = \frac{2B_0}{B_1},$$
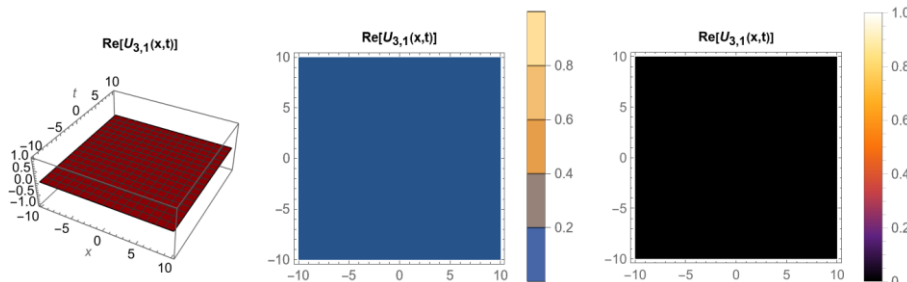
the following solution function is found by means of the coefficients:

$$u_3(x,t) = \frac{i\sqrt{2}ce^{-\vartheta}k(e^{\vartheta}B_0 + B_1)}{\sqrt{b}B_1}. \tag{3.2.4}$$
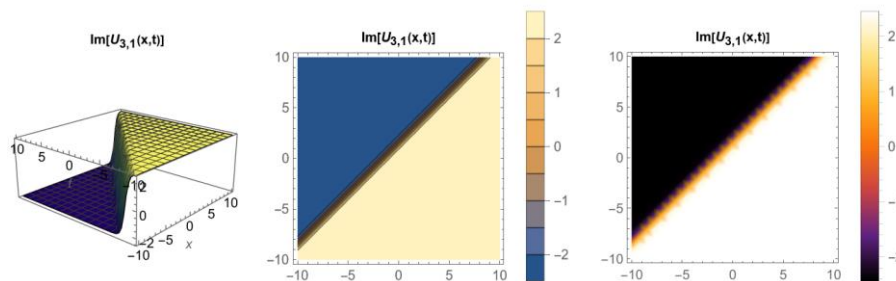
Family 1: For $\lambda^2 - 4\mu > 0$, $\mu \neq 0$ the solution of the equation (3.2.1) and its graphs are:

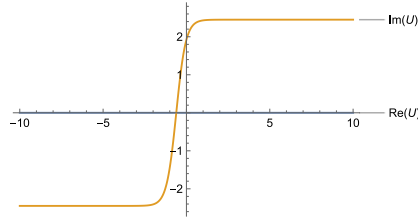$$u_{3,1}(x,t) = \frac{i\sqrt{2}ck(-2\mu B_1 + B_0(\lambda + \rho))}{\sqrt{b}B_1(\lambda + \rho)}, \tag{3.2.5}$$

$$\rho = \left[\sqrt{\lambda^2 - 4\mu}\tanh\left[\frac{1}{2}(E + k(-ct + x))\sqrt{\lambda^2 - 4\mu}\right]\right].$$
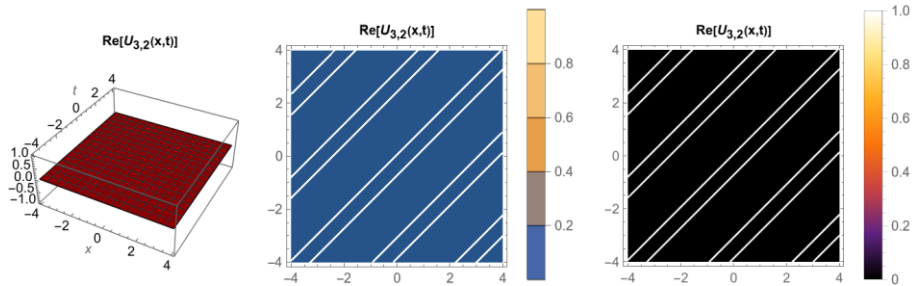

Figure 31. Simulations of the behavior of the model represented by equation (3.2.5) for $B_0 = 2$, $B_1 = 1$, $k = 1$, $c = 1$, $\mu = 1$, $a = 6$, $\lambda = 4$, $b = 1$ and $E = 0.85$

Figure 32. Simulations of the behavior of the model represented by equation (3.2.5) for $B_0 = 2$, $B_1 = 1$, $k = 1$, $c = 1$, $\mu = 1$, $a = 6$, $\lambda = 4$, $b = 1$ and $E = 0.85$
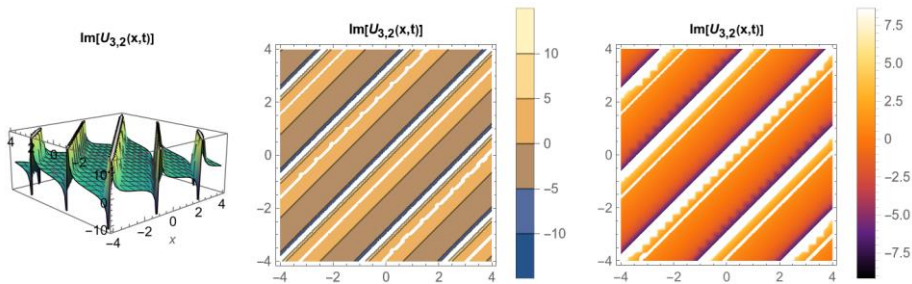
Figure 33. Simulations of the behavior of the model represented by equation (3.2.5) for $B_0 = 2$, $B_1 = 1$, $k = 1$, $c = 1$, $\mu = 1$, $a = 6$, $\lambda = 4$, $b = 1$, $E = 0.85$ and $t = 1$

Family 2: For $\lambda^2 - 4\mu < 0$, $\mu \neq 0$ the solution of the equation (3.2.1) and its graphs are:

$$u_{3,2}(x,t) = \frac{i\sqrt{2}ck\left(-2\mu B_1 + B_0(\lambda - \sigma)\right)}{\sqrt{b}B_1(\lambda - \sigma)}, \tag{3.2.6}$$
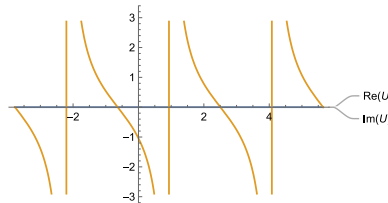
$$\sigma = \left[\sqrt{-\lambda^2 + 4\mu}\tan\left[\frac{1}{2}(E + k(-ct + x))\sqrt{-\lambda^2 + 4\mu}\right]\right].$$

Figure 34. Simulations of the behavior of the model represented by equation (3.2.6) for $B_0 = 1$, $B_1 = 1$, $k = 1$, $c = 1$, $\mu = 2$, $a = -2$, $\lambda = 2$, $b = 1$ and $E = 0.85$
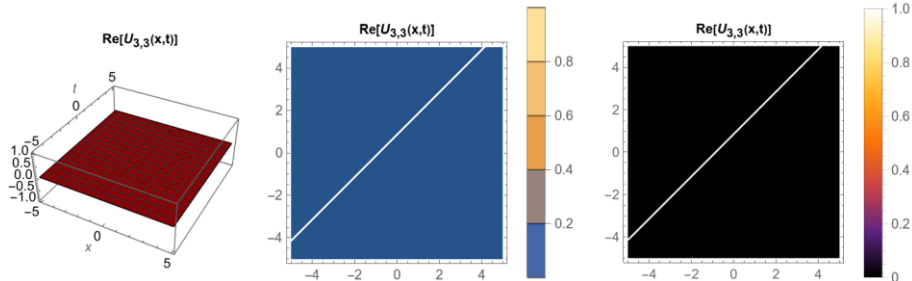

Figure 35. Simulations of the behavior of the model represented by equation (3.2.6) for $B_0 = 1$, $B_1 = 1$, $k = 1$, $c = 1$, $\mu = 2$, $a = -2$, $\lambda = 2$, $b = 1$ and $E = 0.85$
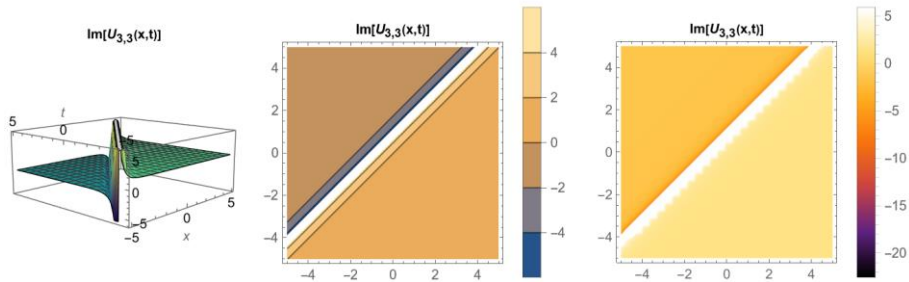

Figure 36. Simulations of the behavior of the model represented by equation (3.2.6) for $B_0 = 1$, $B_1 = 1$, $k = 1$, $c = 1$, $\mu = 2$, $a = -2$, $\lambda = 2$, $b = 1$, $E = 0.85$ and $t = 1$

Family 3: For $\lambda^2 - 4\mu > 0$, $\lambda \neq 0$, $\mu = 0$ the solution of the equation (3.2.1) and its graphs are:
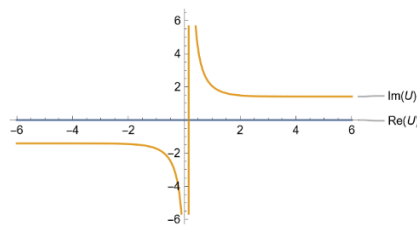
$$u_{3,3}(x,t) = \frac{i\sqrt{2}ck\left(\dfrac{\lambda}{-1 + e^{(E-ckt+kx)\lambda}} + \dfrac{B_0}{B_1}\right)}{\sqrt{b}}. \tag{3.2.7}$$

Figure 37. Simulations of the behavior of the model represented by equation (3.2.7) for $B_0 = 1$, $B_1 = 1$, $k = 1$, $c = 1$, $\mu = 0$, $a = 2$, $\lambda = 2$, $b = 1$ and $E = 0.85$

Figure 38. Simulations of the behavior of the model represented by equation (3.2.7) for $B_0 = 1$, $B_1 = 1$, $k = 1$, $c = 1$, $\mu = 0$, $a = 2$, $\lambda = 2$, $b = 1$ and $E = 0.85$

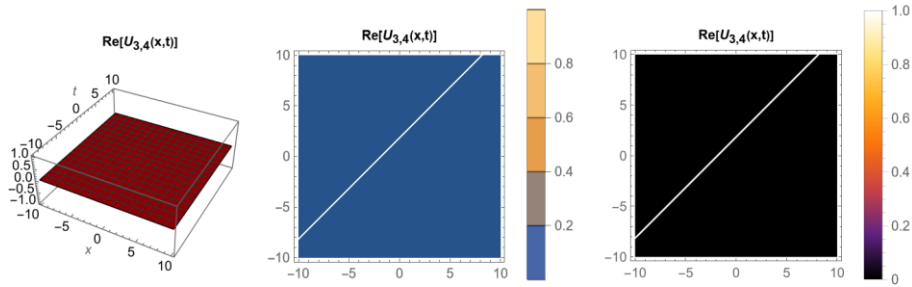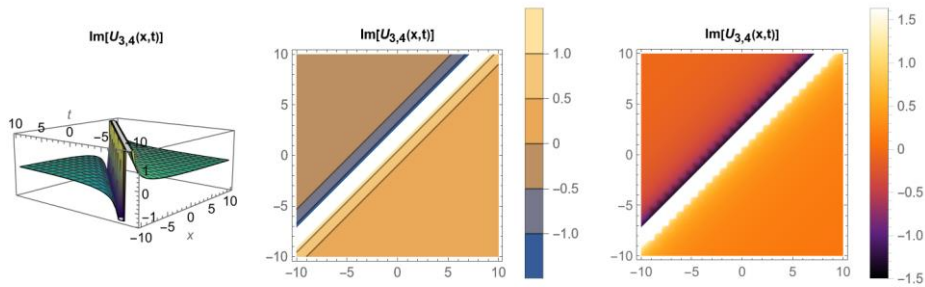

Figure 39. Simulations of the behavior of the model represented by equation (3.2.7) for $B_0 = 1$, $B_1 = 1$, $k = 1$, $c = 1$, $\mu = 0$, $a = 2$, $\lambda = 2$, $b = 1$, $E = 0.85$ and $t = 1$

Family 4: For $\lambda^2 - 4\mu = 0$, $\lambda \neq 0$, $\mu \neq 0$ the solution of the equation (3.2.1) and its graphs are:
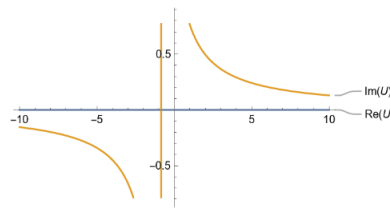
$$u_{3,4}(x,t) = -\frac{i\sqrt{2}ck\left(1 - \dfrac{1}{1 + E - ckt + kx} - \dfrac{B_0}{B_1}\right)}{\sqrt{b}}. \tag{3.2.8}$$

Figure 40. Simulations of the behavior of the model represented by equation (3.2.8) for $B_0 = 1$, $B_1 = 1$, $k = 1$, $c = 1$, $\mu = 1$, $a = 0$, $\lambda = 2$, $b = 1$ and $E = 0.85$

Figure 41. Simulations of the behavior of the model represented by equation (3.2.8) for $B_0 = 1$, $B_1 = 1$, $k = 1$, $c = 1$, $\mu = 1$, $a = 0$, $\lambda = 2$, $b = 1$ and $E = 0.85$
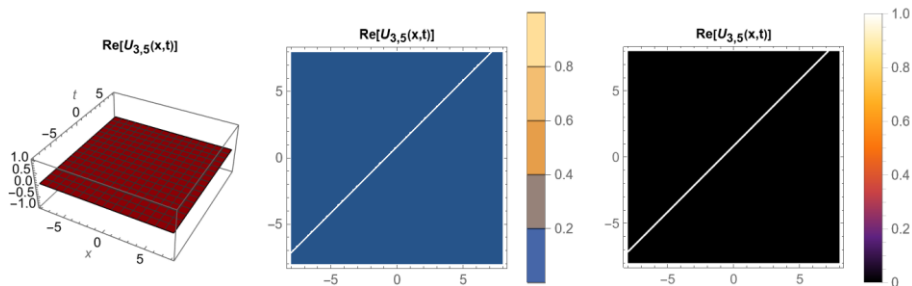

Figure 42. Simulations of the behavior of the model represented by equation (3.2.8) for $B_0 = 1$, $B_1 = 1$, $k = 1$, $c = 1$, $\mu = 1$, $a = 0$, $\lambda = 2$, $b = 1$, $E = 0.85$ and $t = 1$

Family 5: For $\lambda^2 - 4\mu = 0$, $\lambda = 0$, $\mu = 0$ the solution of the equation (3.2.1) and its graphs are:

$$u_{3,5}(x,t) = \frac{i\sqrt{2}ck\left(\left(E + k(-ct + x)\right)B_0 + B_1\right)}{\sqrt{b}\left(E + k(-ct + x)\right)B_1}. \tag{3.2.9}$$
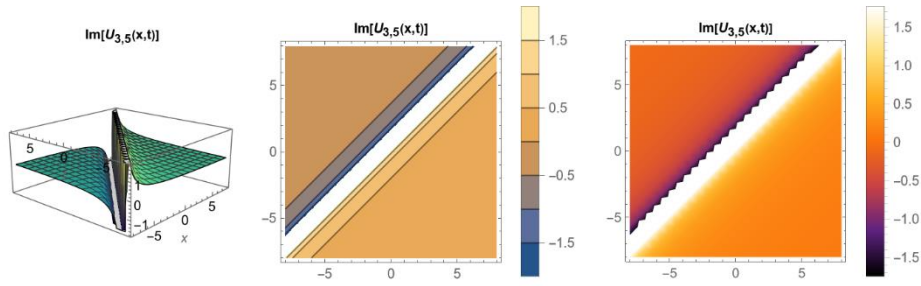

Figure 43. Simulations of the behavior of the model represented by equation (3.2.9) for $B_0 = 0$, $B_1 = 1$, $k = 1$, $c = 1$, $\mu = 0$, $a = 0$, $\lambda = 0$, $b = 1$ and $E = 0.85$

Figure 44. Simulations of the behavior of the model represented by equation (3.2.9) for $B_0 = 0$, $B_1 = 1$, $k = 1$, $c = 1$, $\mu = 0$, $a = 0$, $\lambda = 0$, $b = 1$ and $E = 0.85$
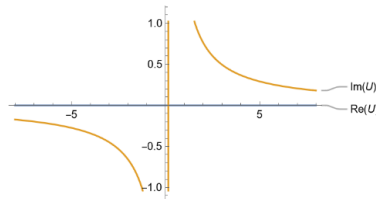
Figure 45. Simulations of the behavior of the model represented by equation (3.2.9) for $B_0 = 0$, $B_1 = 1$, $k = 1$, $c = 1$, $\mu = 0$, $a = 0$, $\lambda = 0$, $b = 1$, $E = 0.85$ and $t = 1$

Case-2:

$$A_0 = -\frac{2c^2k^2B_0^2}{bA_2}, A_1 = -\frac{2i\sqrt{2}ckB_0}{\sqrt{b}}, B_1 = \frac{i\sqrt{b}A_2}{\sqrt{2}ck}, \lambda = -\frac{2i\sqrt{2}ckB_0}{\sqrt{b}A_2}, \mu = -\frac{a}{2c^2k^2} - \frac{2c^2k^2B_0^2}{bA_2^2},$$
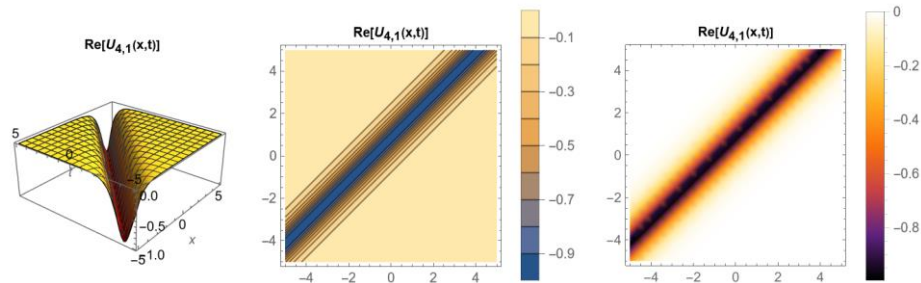
using the coefficients, the following solution function u is reached:

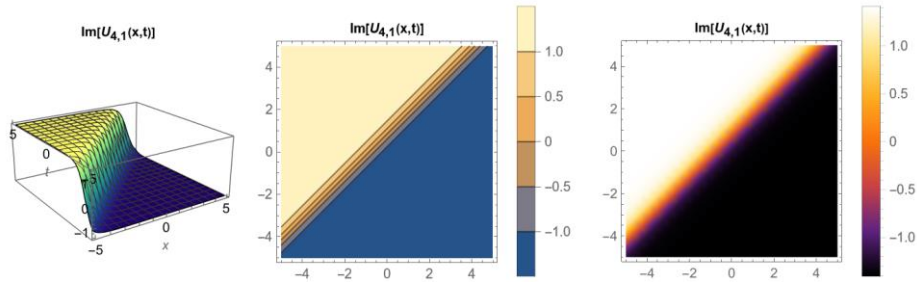$$u_4(x,t) = \frac{ck\left(-i\sqrt{2}\sqrt{b}e^{-\vartheta} - \frac{2ckB_0}{A_2}\right)}{b}. \tag{3.2.10}$$

Family 1: For $\lambda^2 - 4\mu > 0$, $\mu \neq 0$ the solution of the equation (3.2.1) and its graphs are:

$$u_{4,1}(x,t) = \frac{ck\left(-\frac{2ckB_0}{A_2} + \frac{2i\sqrt{2}\sqrt{b}\mu}{\lambda + \rho}\right)}{b}, \tag{3.2.11}$$
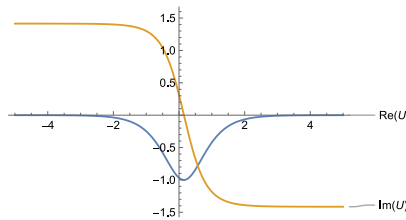
$$\rho = \left[\sqrt{\lambda^2 - 4\mu}\tanh\left[\frac{1}{2}\big(E + k(-ct + x)\big)\sqrt{\lambda^2 - 4\mu}\right]\right].$$

Figure 46. Simulations of the behavior of the model represented by equation (3.2.11) for $B_0 = -1$, $A_2 = 1$, $k = 1$, $c = 1$, $a = 2$, $b = 1$, $\lambda = 2i\sqrt{2}$, $\mu = -3$ and $E = 0.85$

Figure 47. Simulations of the behavior of the model represented by equation (3.2.11) for $B_0 = -1$, $A_2 = 1$, $k = 1$, $c = 1$, $a = 2$, $b = 1$, $\lambda = 2i\sqrt{2}$, $\mu = -3$ and $E = 0.85$

Figure 48. Simulations of the behavior of the model represented by equation (3.2.11) for $B_0 = -1$, $A_2 = 1$, $k = 1$, $c = 1$, $a = 2$, $b = 1$, $\lambda = 2i\sqrt{2}$, $\mu = -3$, $E = 0.85$ and $t = 1$

Family 2: For $\lambda^2 - 4\mu < 0$, $\mu \neq 0$ the solution of the equation (3.2.1) and its graphs are:

$$u_{4,2}(x,t) = \frac{ck\left(-\dfrac{2ckB_0}{A_2} + \dfrac{2i\sqrt{2}\sqrt{b}\mu}{\lambda - \sigma}\right)}{b},$$ (3.2.12)

$$\sigma = \left[\sqrt{-\lambda^2 + 4\mu}\tan\left[\frac{1}{2}\left(E + k(-ct + x)\right)\sqrt{-\lambda^2 + 4\mu}\right]\right].$$
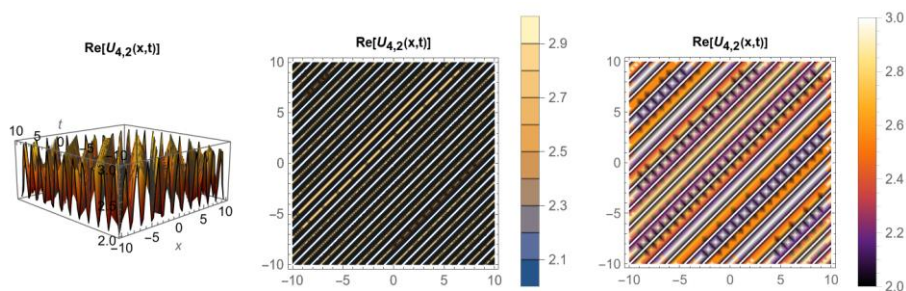

Figure 49. Simulations of the behavior of the model represented by equation (3.2.12) for $B_0 = -1$, $A_2 = 1$, $k = 1$, $c = 1$, $a = -6$, $b = 1$, $\lambda = 2i\sqrt{2}$, $\mu = 1$ and $E = 0.85$

Figure 50. Simulations of the behavior of the model represented by equation (3.2.12) for $B_0 = -1$, $A_2 = 1$, $k = 1$, $c = 1$, $a = -6$, $b = 1$, $\lambda = 2i\sqrt{2}$, $\mu = 1$ and $E = 0.85$

Figure 51. Simulations of the behavior of the model represented by equation (3.2.12) for $B_0 = -1$, $A_2 = 1$, $k = 1$, $c = 1$, $a = -6$, $b = 1$, $\lambda = 2i\sqrt{2}$, $\mu = 1$, $E = 0.85$ and $t = 1$
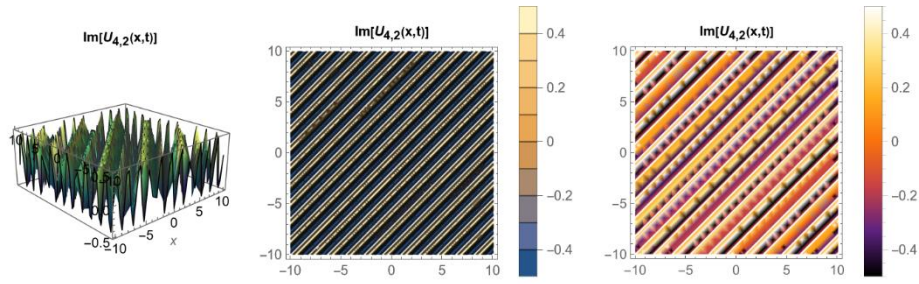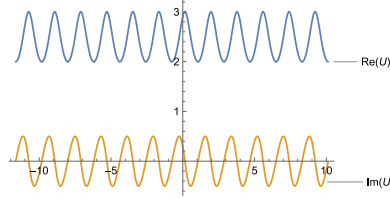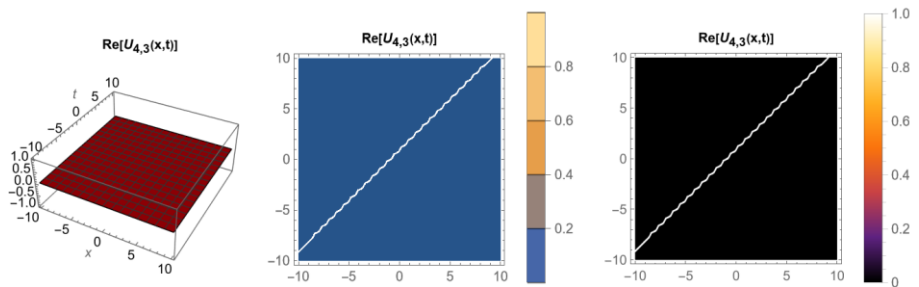
Family 3: For $\lambda^2 - 4\mu > 0$, $\lambda \neq 0$, $\mu = 0$ the solution of the equation (3.2.1) and its graphs are:

$$u_{4,3}(x,t) = \frac{ck\left(-\dfrac{i\sqrt{2}\sqrt{b}\lambda}{-1 + e^{(E-ckt+kx)\lambda}} - \dfrac{2ckB_0}{A_2}\right)}{b}. \tag{3.2.13}$$

Figure 52. Simulations of the behavior of the model represented by equation (3.2.13) for $B_0 = -\sqrt{2}$, $A_2 = i$, $k = 1$, $c = 1$, $a = 8$, $b = 1$, $\lambda = 4$, $\mu = 0$ and $E = 0.85$

Figure 53. Simulations of the behavior of the model represented by equation (3.2.13) for $B_0 = -\sqrt{2}$, $A_2 = i$, $k = 1$, $c = 1$, $a = 8$, $b = 1$, $\lambda = 4$, $\mu = 0$ and $E = 0.85$
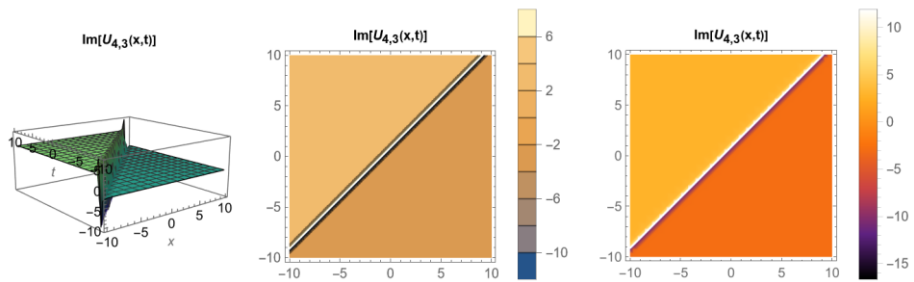
Figure 54. Simulations of the behavior of the model represented by equation (3.2.13) for $B_0 = -\sqrt{2}$, $A_2 = i$, $k = 1$, $c = 1$, $a = 8$, $b = 1$, $\lambda = 4$, $\mu = 0$, $E = 0.85$ and $t = 1$

Family 4: For $\lambda^2 - 4\mu = 0$, $\lambda \neq 0$, $\mu \neq 0$ the solution of the equation (3.2.1) and its graphs are:
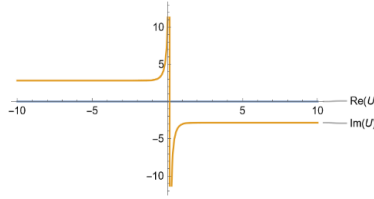
$$u_{4,4}(x,t) = \frac{ck\left(-\dfrac{4\sqrt{2}\sqrt{b}\big(E + k(-ct + x)\big)}{-i + 2E - 2ckt + 2kx} - \dfrac{2ckB_0}{A_2}\right)}{b}. \tag{3.2.14}$$

Figure 55. Simulations of the behavior of the model represented by equation (3.2.14) for $B_0 = -\sqrt{2}$, $A_2 = i$, $k = 1$, $c = 1$, $a = 8$, $b = 1$, $\lambda = 4i, \mu = -4$ and $E = 0.85$

Figure 56. Simulations of the behavior of the model represented by equation (3.2.14) for $B_0 = -\sqrt{2}$, $A_2 = i$, $k = 1$, $c = 1$, $a = 8$, $b = 1$, $\lambda = 4i, \mu = -4$ and $E = 0.85$
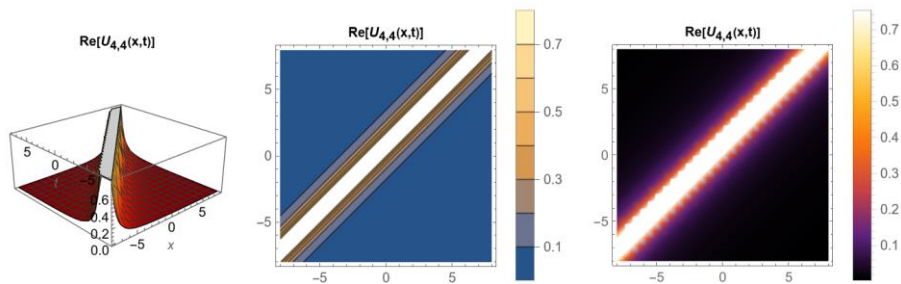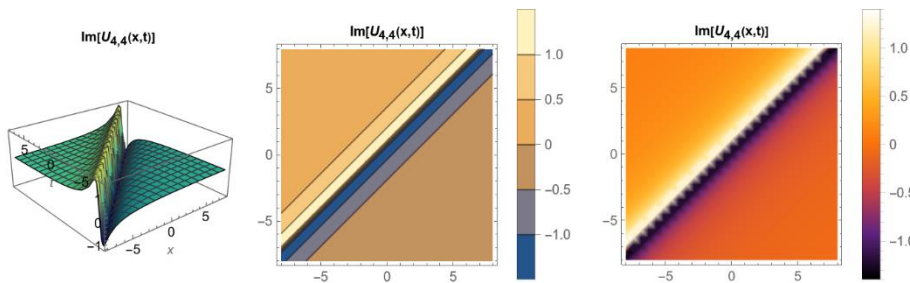

Figure 57. Simulations of the behavior of the model represented by equation (3.2.14) for $B_0 = -\sqrt{2}$, $A_2 = i$, $k = 1$, $c = 1$, $a = 8$, $b = 1$, $\lambda = 4i, \mu = -4$, $E = 0.85$ and $t = 1$

Family 5: For $\lambda^2 - 4\mu = 0$, $\lambda = 0$, $\mu = 0$ the solution of the equation (3.2.1) and its graphs are:
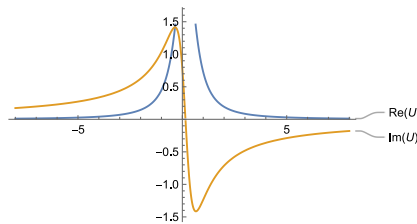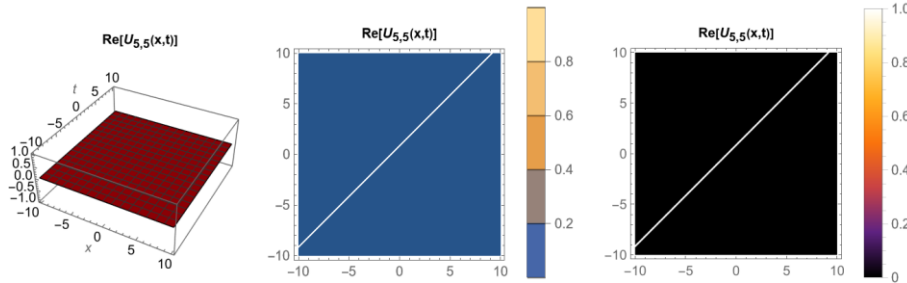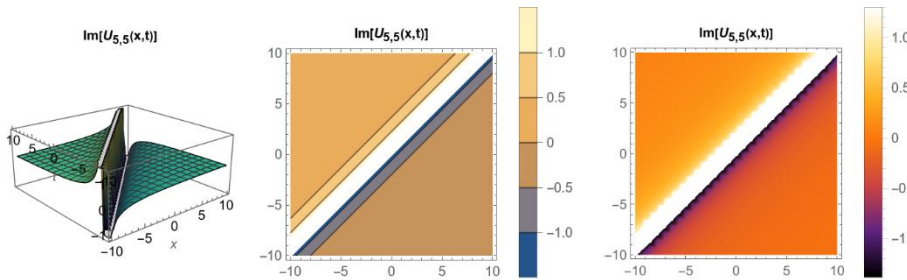
$$u_{4,5}(x,t) = \frac{ck\left(-\dfrac{i\sqrt{2}\sqrt{b}}{E + k(-ct + x)} - \dfrac{2ckB_0}{A_2}\right)}{b}.$$

(3.2.15)

Figure 58. Simulations of the behavior of the model represented by equation (3.2.15) for $B_0 = 0$, $A_2 = 1$, $k = 1$, $c = 1$, $a = 0$, $b = 1$, $\lambda = 0$, $\mu = 0$ and $E = 0.85$

Figure 59. Simulations of the behavior of the model represented by equation (3.2.15) for $B_0 = 0$, $A_2 = 1$, $k = 1$, $c = 1$, $a = 0$, $b = 1$, $\lambda = 0$, $\mu = 0$ and $E = 0.85$
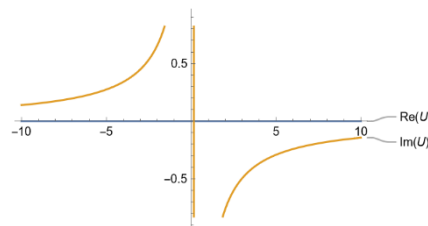
Figure 60. Simulations of the behavior of the model represented by equation (3.2.15) for $B_0 = 0$, $A_2 = 1$, $k = 1$, $c = 1$, $a = 0$, $b = 1$, $\lambda = 0$, $\mu = 0$, $E = 0.85$ and $t = 1$

5. Conclusion

This paper applied the modified exponential function method to the (1+1)-dimensional Landau-Ginzburg-Higgs and Duffing nonlinear partial differential equations to reach and analyze the traveling wave solutions. The solution functions of the (1+1)-dimensional Landau-Ginzburg-Higgs equation, in case-1 and case-2, family 1, family 2 and family 3 are hyperbolic, trigonometric and exponential functions and show periodic properties. Again in case-1 and case-2, family 4 and family 5 rational solutions have been get. In the solutions of the Duffing equation, hyperbolic, trigonometric and exponential functions

were reached in case-1 and case-2, family 1, family 2 and family 3. These solution functions also have periodic properties. In case-1 and case-2, family 4 and family 5 are found to be rational functions. It is an important point in interpreting the behavior of the wave motion, especially in understanding the physical phenomenon behind the two models discussed, to achieve periodic solution functions with the help of appropriate wave transform. In the literature, the solutions of these equations have been obtained by using various methods. In this study, it has been observed that the solution functions get with the modified exponential function method are different and new. By giving the appropriate parameters to the solution functions found, simulations of the behavior of the mathematical model as three-dimensional, contour, density and two-dimensional graphics were get with the help of the package program. Thus, it provided a prospective advantage for researchers to physically interpret the behavior of these two important mathematical models. As a result, it is emphasized that the modified exponential function method is an effective method in investigating the solutions of nonlinear partial differential equations, which is an example of mathematical modeling.

References

[1]   Liu, C. S., Trial equation method and its applications to nonlinear evolution equations, **Acta Physica Sinica**, **54**, 6, 2505-2509, (2005).

[2]   Hammouch, Z., Yavuz, M. and Özdemir, N., Numerical solutions and synchronization of a variable-order fractional chaotic system. **Mathematical Modelling and Numerical Simulation with Applications**, **1**, 1, 11-23, (2021).

[3]   Hosseini, K. and Ansari, R., New exact solutions of nonlinear conformable time-fractional Boussinesq equations using the modified Kudryashov method, **Waves in Random and Complex Media**, **27**, 4, 628-636, (2017).

[4]   Baskonus, H. M., Bulut, H. and Sulaiman, T.A., Investigation of various travelling wave solutions to the extended (2+ 1)-dimensional quantum ZK equation, **The European Physical Journal Plus**, **132**, 11, 1-8, (2017).

[5]   Wazwaz, A.M., The tanh method for traveling wave solutions of nonlinear equations, **Applied Mathematics and Computation**, **154**, 3, 713-723, (2004).

[6]   Evirgen, F., Analyze the optimal solutions of optimization problems by means of fractional gradient based system using VIM, **An International Journal of Optimization and Control: Theories & Applications (IJOCTA), 6**, 2, 75-83, (2016).

[7]   He, J. H. and Wu, X. H., Exp-function method for nonlinear wave equations, **Chaos, Solitons & Fractals**, **30**, 3, 700-708, (2006).

[8]   Barman, H. K., Akbar, M. A., Osman, M. S., Nisar, K. S., Zakarya, M., Abdel-Aty, A. H. and Eleuch, H., Solutions to the Konopelchenko-Dubrovsky equation and the Landau-Ginzburg-Higgs equation via the generalized Kudryashov technique, **Results in Physics**, **24**, 104092, (2021).

[9]   Eze, E. O., Obasi, U. E. and Agwu, E. U., Stability Analysis of Periodic Solutions of Some Duffing's Equations, **Open Journal of Applied Sciences**, **9**, 4, 198-214, (2019).

[10]   Naher, H. and Abdullah, F. A., New approach of (G′/G)-expansion method and new approach of generalized (G′/G)-expansion method for nonlinear evolution equation, **AIP Advances**, **3**, 3, 032116, (2013).

[11] Islam, M. E. and Akbar, M. A., Stable wave solutions to the Landau-Ginzburg-Higgs equation and the modified equal width wave equation using the IBSEF method, **Arab Journal of Basic and Applied Sciences**, 27, 1, 270-278, (2020).

[12] Bekir, A. and Unsal, O., Exact solutions for a class of nonlinear wave equations by using first integral method, **International Journal of Nonlinear Science**, **15**, 2, 99-110, (2013).

[13] Evans, D. J. and Raslan, K. R., The tanh function method for solving some important non-linear partial differential equations, **International Journal of Computer Mathematics**, **82**, 7, 897-905, (2005a).

[14] Hu, W. P., Deng, Z. C., Han, S. M. and Fa, W., Multi-symplectic Runge-Kutta methods for Landau-Ginzburg-Higgs equation, **Applied Mathematics and Mechanics**, **30**, 8, 1027-1034, (2009).

[15] Iftikhar, A., Ghafoor, A., Zubair, T., Firdous, S. and Mohyud-Din, S. T., -expansion method for traveling wave solutions of (2+ 1) dimensional generalized KdV, Sin Gordon and Landau-Ginzburg-Higgs Equations, **Scientific Research and Essays**, **8**, 28, 1349-1359, (2013).

[16] Cevikel, A. C., Aksoy, E., Günerb, Ö. and Bekir, A., Dark-bright soliton solutions for some evolution equations, **International Journal of Nonlinear Science**, **16**, 3, 195-202, (2013).

[17] Salas, A. H., Exact solution to Duffing equation and the pendulum equation, **Applied Mathematical Sciences**, **8**, 176, 8781-8789, (2014).

[18] Al-Jawary, M. A. and Abd-Al-Razaq, S. G., Analytic and numerical solution for Duffing equations, **International Journal of Basic and Applied Sciences**, **5**, 2, 115-119, (2016).

[19] Akbar, M. A. and Ali, N. H. M., Exp-function method for Duffing equation and new solutions of (2+ 1) dimensional dispersive long wave equations, **Progress in Applied Mathematics**, **1**, 2, 30-42, (2011).

[20] Bülbül, B. and Sezer, M., Numerical solution of Duffing equation by using an improved Taylor matrix method, **Journal of Applied Mathematics**, (2013).

[21] Marinca, V. and Herişanu, N., Explicit and exact solutions to cubic Duffing and double-well Duffing equations, **Mathematical and Computer Modelling**, **53**, 5-6, 604-609, (2011).

[22] Tabatabaei, K. and Gunerhan, E., Numerical solution of Duffing equation by the differential transform method, **Applied Mathematics & Information Sciences Letters**, **2**, 1, 1-6, (2014).